High Saturation Power and High Gain Integrated Photoreceivers

Anna Tauke-Pedretti, *Student Member, IEEE*, Matthew Dummer, *Student Member, IEEE*, Jonathon S. Barton, *Member, IEEE*, Matthew N. Sysak, *Student Member, IEEE*, James W. Raring, *Student Member, IEEE*, and Larry A. Coldren, *Fellow, IEEE*

***Abstract*—A novel monolithically integrated semiconductor optical amplifier (SOA) receiver is presented. This receiver implements a flared SOA and tapered quantum-well detector. SOAs exhibited 22-dB unsaturated gain and 15.7-dBm output power at the 1-dB gain compression point while the receiver demonstrated 15-GHz bandwidth and −10.5-dBm sensitivity.**

***Index Terms*—Offset quantum well, optical receivers, saturation power, semiconductor optical amplifiers (SOAs), waveguide photodiodes, wavelength conversion.**

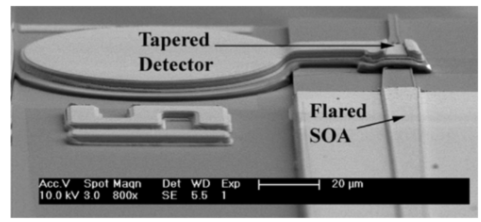

Fig. 1. Scanning electron microscope (SEM) of integrated photoreceiver.

I. Introduction

Monolithically integrated photoreceivers which combine amplification and detection elements are advantageous over discrete devices by producing greater sensitivity, decreased coupling loss, simplified packaging, and reduced cost. Although high performance semiconductor optical amplifier (SOA)-PINs have been fabricated with bandwidths up to 40 GHz, typically they produce low output powers (~ 200 mV$_{p\text{-}p}$) requiring the signal to be electronically amplified for many applications [1], [2].

As optical device integration density continues to increase, it becomes desirable to develop integration platforms that are compatible with tunable lasers as well as receivers. One such photonic integrated circuit of interest is a photocurrent driven wavelength converter. These devices use photocurrent from detected input light to drive optical modulators. For size and packaging considerations of wavelength converters, it is desirable to monolithically integrate the receivers and transmitters, thus constraining the material used to be compatible with the fabrication of lasers. To maintain small footprints and minimize parasitic effects in monolithic wavelength converters, it is beneficial to avoid the use of electrical amplification. In past devices, the conversion efficiency and the extinction of the converted signal have been limited by the gain and low saturation powers of the photoreceiver used [3], [4]. These limitations can be overcome with the use of the photoreceivers presented in this letter [5].

Waveguide photodetectors allow for efficient detection of light and are easy to integrate with SOAs; however, they often suffer from saturation problems and degrade at high optical powers due to the high optical power density/photocurrent at the front end of the detector. The detector presented here achieves acceptable power densities at the front end and minimum capacitance through the use of lateral tapering.

It is well known that the high optical power density in SOAs will deplete active region carriers creating gain saturation. When modulated light is amplified, it is desirable to operate at power levels below saturation to prevent signal distortion. The saturation power levels can be increased through gain clamping, reducing the power density [6], or increasing carrier density [7]. In this letter, the SOA has been laterally flared to keep the optical power density below saturation while the power grows.

II. Device

The photoreceiver consists of a monolithically integrated SOA and quantum-well absorber, as shown in Fig. 1.

The SOA is designed as a two-stage amplifier. A 200-μm-long by 3-μm-wide section provides gain to low input powers while keeping amplified spontaneous emission noise to a minimum. This is followed by a 400-μm-long section, which linearly flares from 3 to 9 μm. The flaring is implemented to reduce the optical power density, thus increasing the SOA saturation power. The 50-μm-long photodetector employs a linear ridge taper from 9 to 3 μm to prevent front-end saturation effects at high optical powers. Photo-bis-benzocyclobutene (BCB) is used under the detector pads in order to reduce the parasitic pad capacitance.

The device is fabricated using an offset quantum-well material structure with a single regrowth. The fabrication process is completely compatible with that of a sampled-grating distributed-Bragg-reflector transmitter and requires no additional steps [3]–[5]. A curved and flared input waveguide is used to aid in fiber coupling as well as to reduce optical reflections. In addition, a multilayer antireflection coating is applied to further reduce the optical reflections. Seven quantum wells provide the

Manuscript received January 19, 2005; revised June 2, 2005. This work was supported by Intel Corporation Grant TXA001630000 and by Defense Advanced Research Projects Agency (DARPA) MTO-LASOR Grant W911NF-04-9-0001.

The authors are with the Department of Electrical Engineering and the Department of Materials Engineering, University of California Santa Barbara, Santa Barbara, CA 93106 USA (e-mail: atauke@engineering.ucsb.edu; dummer@engineering.ucsb.edu; jsbarton@engineering.ucsb.edu; mnsysak@engineering.ucsb.edu; jraring@engineering.ucsb.edu; coldren@ece.ucsb.edu).

Digital Object Identifier 10.1109/LPT.2005.854422

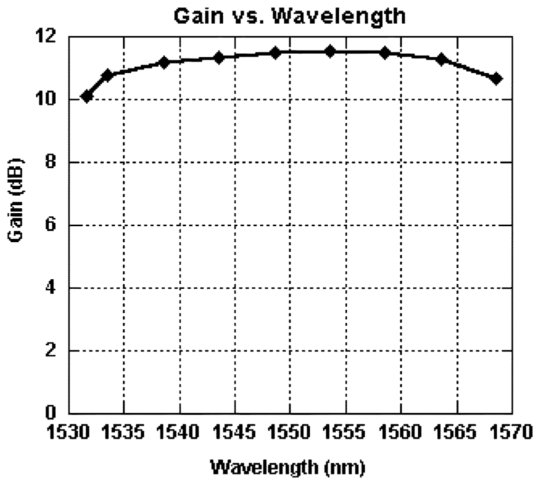

Fig. 2. Gain versus wavelength plot for receiver. ($I_{\mathrm{SOA}} = 250$ mA (8.33 kA/cm^2), $V_{\mathrm{detector}} = -4$ V, and $P_{\mathrm{in}} = 0.8$ mW).

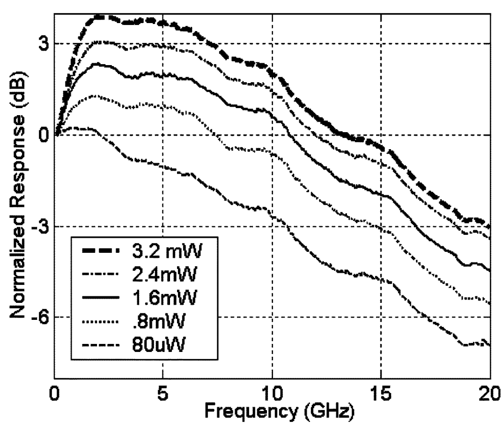

Fig. 3. Input power dependence of the frequency response of the receiver. ($I_{\mathrm{SOA}} = 250$ mA (8.33 kA/cm^2) and $V_{\mathrm{detector}} = -4$ V).

gain for the forward-biased SOA and the same wells provide a high absorption coefficient in the reverse biased detector.

III. Results

The devices were thinned, cleaved, and mounted onto an aluminum nitride carrier for testing. All dc contacts were wirebonded to the carrier and contacted via a probe card. The detector was directly probed by a coplanar stripline probe to prevent any parasitic effects from wirebonds. In all cases, input powers quoted were for light coupled into the waveguide. The compressively strained quantum wells used in this device are highly polarization-dependent; therefore, the polarization was adjusted to transverse electric to allow for maximum gain during all measurements. This polarization dependence is typical of devices that implement strained quantum wells and can be eliminated with redesigned quantum wells or bulk active material [2].

The dependence of dc gain on wavelength was measured. As shown in Fig. 2, the device exhibited less than 1.5-dB gain variation between 1530 and 1570 nm. This wavelength dependence can be attributed to the optical bandwidth of the quantum wells used for gain in the SOA and absorption in the detector.

The radio-frequency (RF) characteristics of the receiver were also measured. For all measurements, the input wavelength was

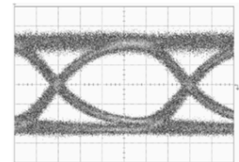

Fig. 4. 20-Gb/s eye for 2^{31}-1 pseudorandom binary sequence (PRBS). ($I_{\mathrm{SOA}} = 250$ mA, $V_{\mathrm{detector}} = -5$ V, and $P_{\mathrm{in}} = 0.8$ mW).

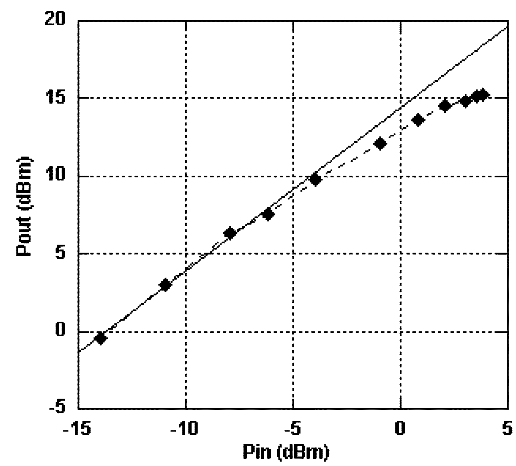

Fig. 5. Optical P_{in} versus optical $P_{\mathrm{out}} \propto I_{\mathrm{photocurrent}}$ at 10 Gb/s. ($I_{\mathrm{SOA}} = 250$ mA (8.33 kA/cm^2) and $V_{\mathrm{detector}} = -4$ V).

1548.1 nm and the detector was terminated with 50 Ω. The device has demonstrated a 3-dB bandwidth of 15 GHz for Pin = 0.8 mW (Fig. 3). It is believed the frequency response peaking between 1 and 5 GHz is caused by the input optical signal modulating the carrier density when the SOA experiences gain saturation. Similar peaking was also seen in the frequency response of electrically modulated gain-saturated SOAs [8]. Typically, photodetector saturation will manifest itself through a steeper bandwidth rolloff for high powers. In this case, there was no bandwidth degradation, thus confirming unsaturated photodetector operation. The 20-Gb/s eye diagrams were open and lacking pattern dependence (Fig. 4).

Greater than 14 dB of optical gain was realized at 10-Gb/s operation and the 1-dB gain compression point was reached at 12 dBm of output power (Fig. 5). This translates into ~16 mA of unsaturated photocurrent, which allows for unsaturated voltage swings up to 0.8 $V_{p\text{-}p}$ when terminated with 50 Ω. It should be noted the RF gain was slightly higher than the dc gain due to additional heating effects at dc.

Bit-error-rate (BER) testing at 10 Gb/s with a nonreturn-to-zero 2^{31}-1 pseudorandom bit sequence was used to demonstrate the -10.5-dBm sensitivity of the receiver (Fig. 6). The BER testing utilized a 10-Gb/s transmitter (Agilent 83 433A) at a wavelength of 1548.1 nm. The signal from the transmitter went through a high power erbium-doped fiber amplifier followed by a polarization controller, an optical filter, and finally an attenuator before being coupled into the device.

The receiver is less sensitive than the -17-dBm sensitivity reported for similar devices in literature [1]. The wider ridge of the receiver presented here is necessary to improve the saturation power; however, this also increases the spontaneous emission therefore limiting the device's sensitivity.

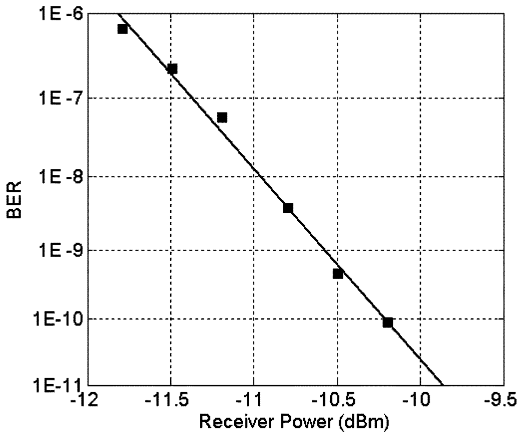

Fig. 6. BER curve for a input signal at 10 Gb/s and 2^{31}-1 PRBS. ($I_{\rm SOA}$ = 200 mA and $V_{\rm detector} = -5$ V).

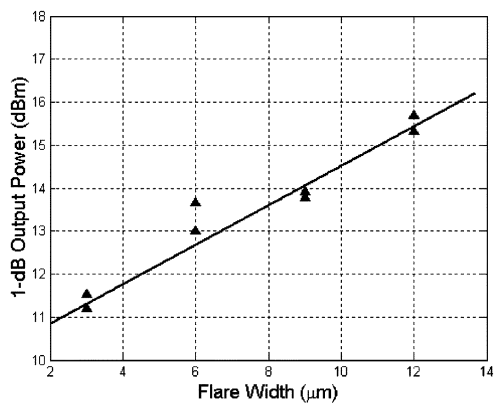

Fig. 7. Output power for 1-dB gain compression point versus the final flare width. ($J_{\rm SOA} = 8.33$ kA/cm^2).

IV. Design Studies

To aid in future receiver designs, the effects of SOA length and flare width have been examined. The SOAs studied were identical to the receiver's SOA except for variations in the length or flare width. These SOAs were integrated with detectors and characterized with dc testing.

The SOAs demonstrated a linear dependence of output saturation power with flare width (Fig. 7). A maximum 1-dB compression point of 15.7 dBm was achieved with a 12-μm flare width.

Gain versus length was characterized for straight 3-μm-wide SOAs. The unsaturated gain for different lengths and current densities was measured with the integrated detector. This data shows excellent linearity with length achieving up to 22 dB of gain, as shown in Fig. 8.

V. Conclusion

A monolithically integrated photoreceiver has been successfully fabricated on a simple offset quantum-well platform requiring only a single regrowth. The 600-μm-long flared SOA has produced greater than 14 dB of gain and 1-dB output saturation power of 12 dBm. However, additional design studies have indicated that improvements in the SOA saturation power and

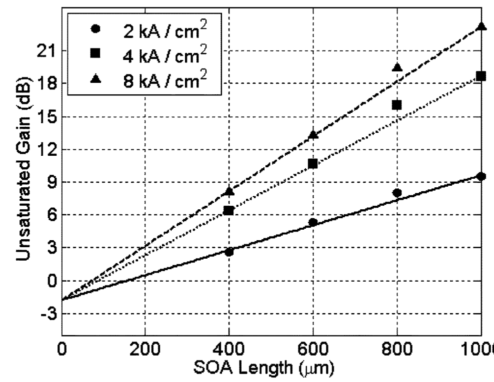

Fig. 8. Unsaturated gain versus length for three different current densities.

gain are possible. The tapered photodetector biased at -4 V has shown no signs of saturation and has demonstrated a 15-GHz bandwidth and a sensitivity of -10.5 dBm. In conclusion, the high saturation power and significant gain of these receivers make them an excellent choice for the photocurrent driven wavelength converter as well as other applications.

Acknowledgment

The authors would like to acknowledge C. Wang for SEM images and Agility Communications for antireflection coatings.

References

[1] B. Mason, J. M. Geary, J. M. Freund, A. Ougazzaden, C. Lentz, K. Glogovsky, G. Przybylek, L. Peticolas, F. Walters, L. Reynolds, J. Boardman, T. Kercher, M. Rader, D. Monroe, and L. Ketelsen, "40 Gb/s photonic integrated receiver with -17 dBm sensitivity," in *Optical Fiber Communications (OFC 2002)*, vol. 2, Mar. 17–22, 2002, Postdeadline Papers, pp. FB10-1–3.

[2] D. Wake, S. N. Judge, T. P. Spooner, M. J. Harlow, W. J. Duncan, I. D. Henning, and M. J. O'Mahony, "Monolithic integration of 1.5 μm optical preamplifier and PIN photodetector with a gain of 20 dB and a bandwidth of 35 GHz," *Electron. Lett.*, vol. 26, pp. 1166–1168, Jul. 1990.

[3] M. N. Sysak, J. S. Barton, L. A. Johansson, J. W. Raring, E. J. Skogen, M. L. Masanovic, D. J. Blumenthal, and L. A. Coldren, "Single-chip wavelength conversion using a photocurrent-driven EAM integrated with a widely tunable sampled-grating DBR laser," *IEEE Photon. Technol. Lett.*, vol. 16, no. 9, pp. 2093–2095, Sep. 2004.

[4] J. S. Barton, M. L. Masanovic, M. N. Sysak, J. M. Hutchinson, E. J. Skogen, D. J. Blumenthal, and L. A. Coldren, "2.5-Gb/s error-free wavelength conversion using a monolithically integrated widely tunable SGDBR-SOA-MZ transmitter and integrated photodetector," *IEEE Photon. Technol. Lett.*, vol. 16, no. 6, pp. 1531–1533, Jun. 2004.

[5] J. S. Barton, A. Tauke-Pedretti, M. Dummer, M. N. Sysak, M. L. Masanovic, J. Raring, E. J. Skogen, and L. A. Coldren, "10 Gbit/s wavelength conversion using a widely-tunable series push-pull photocurrent-driven transmitter," *IEEE Photon. Technol. Lett.*, vol. 17, no. 9, pp. 1902–1904, Sep. 2005.

[6] M. Connelly, *Semiconductor Optical Amplifiers*. Boston, MA: Kluwer Academic, 2002, ch. 2–3.

[7] S. S. Saini, J. Bowser, R. Enck, V. Luciani, P. J. S. Helm, and M. Dagenais, "A semiconductor optical amplifier with high saturation power, low noise figure and low polarization dependent gain over the C-band," in *17th Annu. Meeting IEEE Lasers and Electro-Optics Society (LEOS 2004)*, vol. 1, Nov. 8–9, 2004, pp. 102–103.

[8] L. San-Liang, M. E. Heimbuch, D. A. Cohen, L. A. Coldren, and S. P. DenBaars, "Integration of semiconductor laser amplifiers with sampled grating tunable lasers for WDM applications," *IEEE J. Sel. Topics Quantum Electron.*, vol. 3, no. 2, pp. 615–27, Apr. 1997.